



UNIVERSITY OF LEEDS

This is a repository copy of *Non-Functionalized Ultrasmall Silica Nanoparticles Directly and Size-Selectively Activate T Cells*.

White Rose Research Online URL for this paper:
<http://eprints.whiterose.ac.uk/139449/>

Version: Supplemental Material

Article:

Vis, B, Hewitt, RE, Faria, N et al. (6 more authors) (2018) Non-Functionalized Ultrasmall Silica Nanoparticles Directly and Size-Selectively Activate T Cells. *ACS Nano*, 12 (11). pp. 10843-10854. ISSN 1936-0851

<https://doi.org/10.1021/acsnano.8b03363>

© 2018 American Chemical Society. This is an author produced version of a paper published in *ACS Nano*. Uploaded in accordance with the publisher's self-archiving policy.

Reuse

Items deposited in White Rose Research Online are protected by copyright, with all rights reserved unless indicated otherwise. They may be downloaded and/or printed for private study, or other acts as permitted by national copyright laws. The publisher or other rights holders may allow further reproduction and re-use of the full text version. This is indicated by the licence information on the White Rose Research Online record for the item.

Takedown

If you consider content in White Rose Research Online to be in breach of UK law, please notify us by emailing eprints@whiterose.ac.uk including the URL of the record and the reason for the withdrawal request.



eprints@whiterose.ac.uk
<https://eprints.whiterose.ac.uk/>

Non-Functionalized Ultrasmall Silica Nanoparticles Directly and Size-Selectively Activate T Cells

Authors: Bradley Vis^{†‡§*}, Rachel E. Hewitt^{†‡*}, Nuno Faria^{†‡}, Carlos Bastos^{†‡}, Helen Chappell^{†‡Φ},
Laetitia Pele^{†‡}, Ravin Jugdaohsingh^{†‡}, Stephen D. Kinrade[§], Jonathan J. Powell^{†‡}

[†]Biomaterial Research Group, Department of Veterinary Medicine, University of Cambridge, Madingley Road, Cambridge CB3 0ES, UK.

[‡]Biomaterial Research Group, Department of Mineral Science and Technology, MRC Elsie Widdowson Laboratory, Fulbourn Road, Cambridge CB1 9NL, UK.

[§]Department of Chemistry, Lakehead University, 955 Oliver Road, Thunder Bay, Ontario P7B 5E1, Canada.

^ΦSchool of Food Science and Nutrition, University of Leeds, Woodhouse Lane, Leeds, LS2 9JT, UK

*Equal contributors

Corresponding author: Jonathan Powell. jjp37@cam.ac.uk

Figure S1.

Model of a 2.9 nm USSN derived from the manual packing of a previous DFT-optimised model of a $(\text{SiO}_2)_{24}$ cluster.¹ The original small clusters were simulated in a hydrated environment and represent the lowest energy state. However, no further relaxation was carried out on the larger particle and a hydration shell was not included. (A 0.35 nm hydration shell would increase the hydrated particle size to 3.6 nm for example).

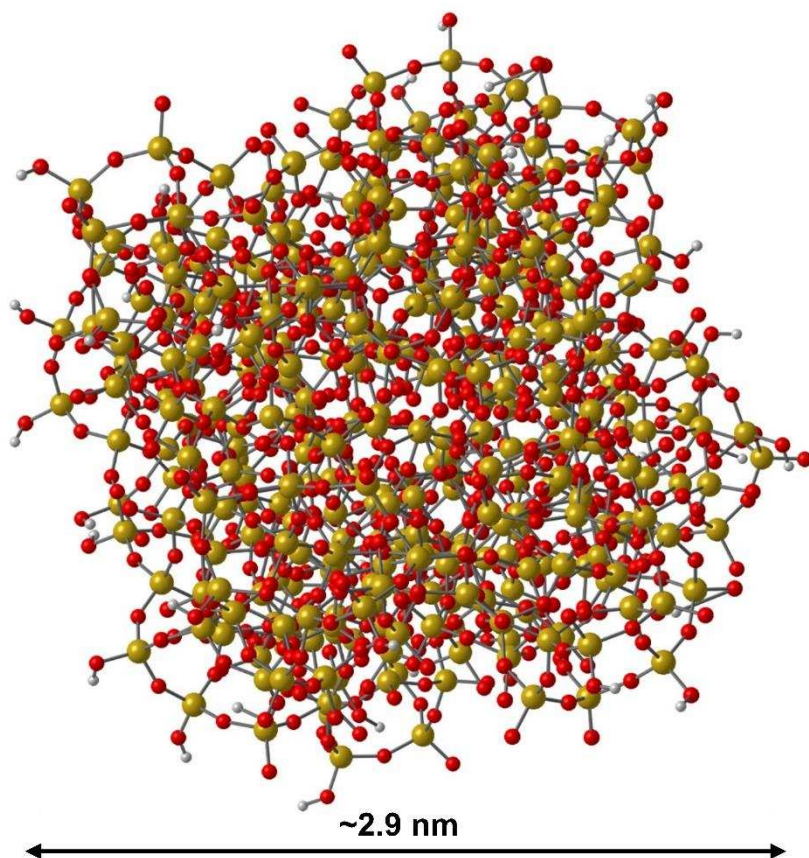


Figure S2.

IL-1 β levels in PBMC supernatants after 3 h treatment challenge followed by a 21 h incubation. PBMC cultures were unstimulated or stimulated with 10 ng/mL lipopolysaccharide for 3 h prior to challenge with silica. Data are reported as means \pm standard deviation for 4 replicates. * denotes significance against the control ($p < 0.05$, one-way ANOVA).

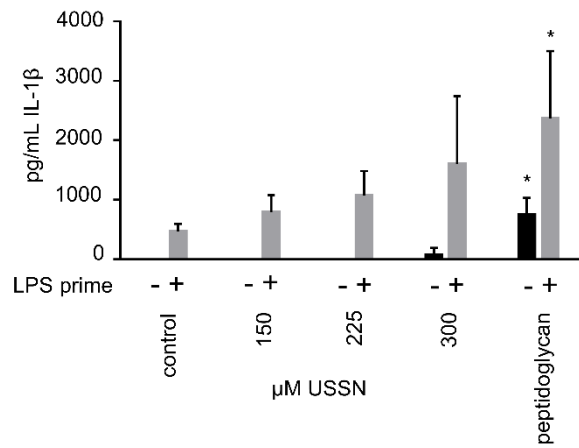


Figure S3

Dissolution of 800 μM USSNs in cell-free growth media at 37 °C. The percentage of dissolved silica was determined through ultrafiltration (<3 kDa). Means \pm standard deviation for 6 replicates.

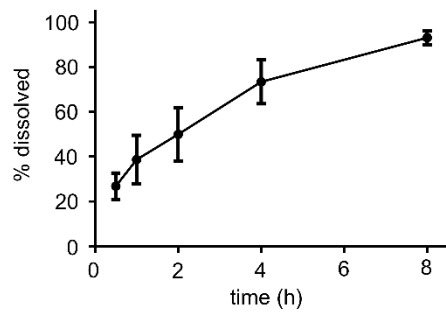


Figure S4. The cell distribution in enriched T cell cultures.

Cells were first selected based on generous FSC versus SSC profiles that also excluded debris, followed by T cell (CD3), and subsequent monocyte (CD11c), B cell (CD19) and unstained (CD3(-)CD11c(-)(CD19(-)) gates.

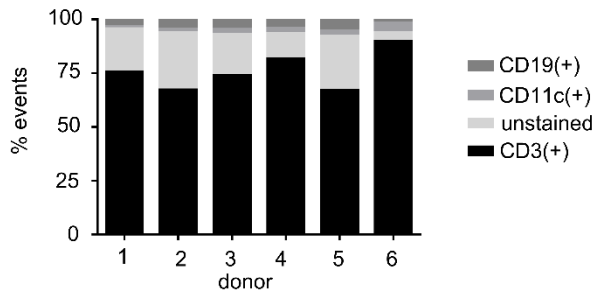


Figure S5. Gating strategy employed for assessing CD25 and CD69 on CD4 and CD8 T cells in PBMC culture.

Cells were first selected based on a T cell FSC versus SSC profile that also excluded debris, followed by a viable T cell (CD3(+)), and a CD4(+) or CD8(+) gate. Percentage of cells positive for CD25 and CD69 were assessed through quadrant gating, and mean fluorescent intensity for the activation markers was recorded.

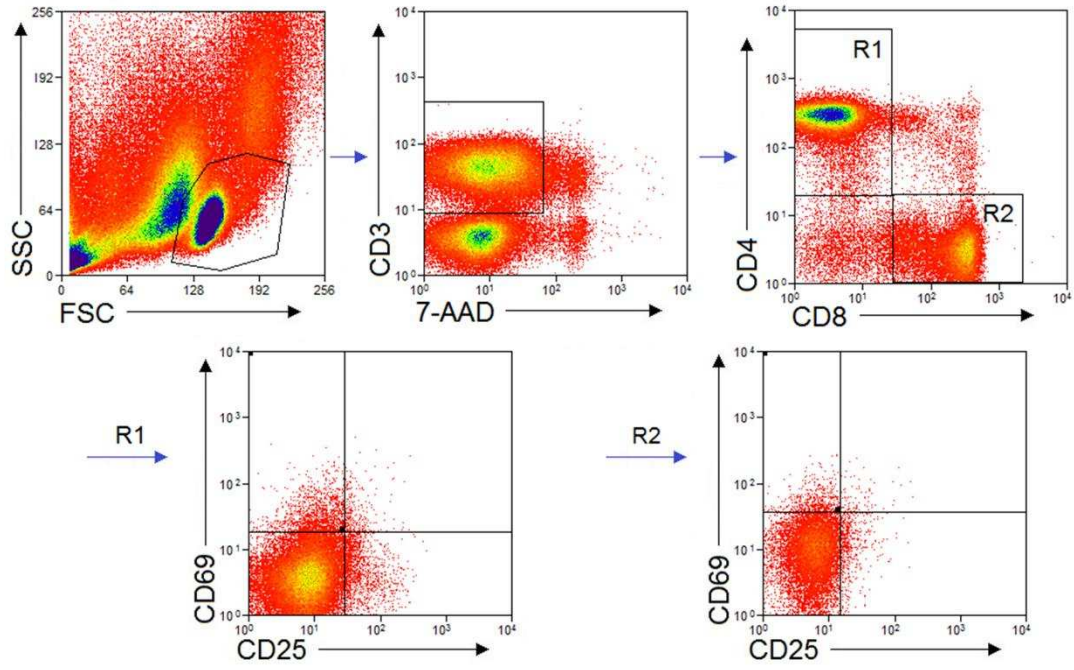


Figure S6. Gating strategy employed for assessing proliferation of CD4 and CD8 T cells in PBMC culture

Cells were first selected based on a T cell FSC versus SSC profile that also excluded debris, followed by a viable T cell (CD3(+)), and a CD4(+) or CD8(+) gate. Percentage of cells divided was assessed through CFDA-SE^{LOW} gate.

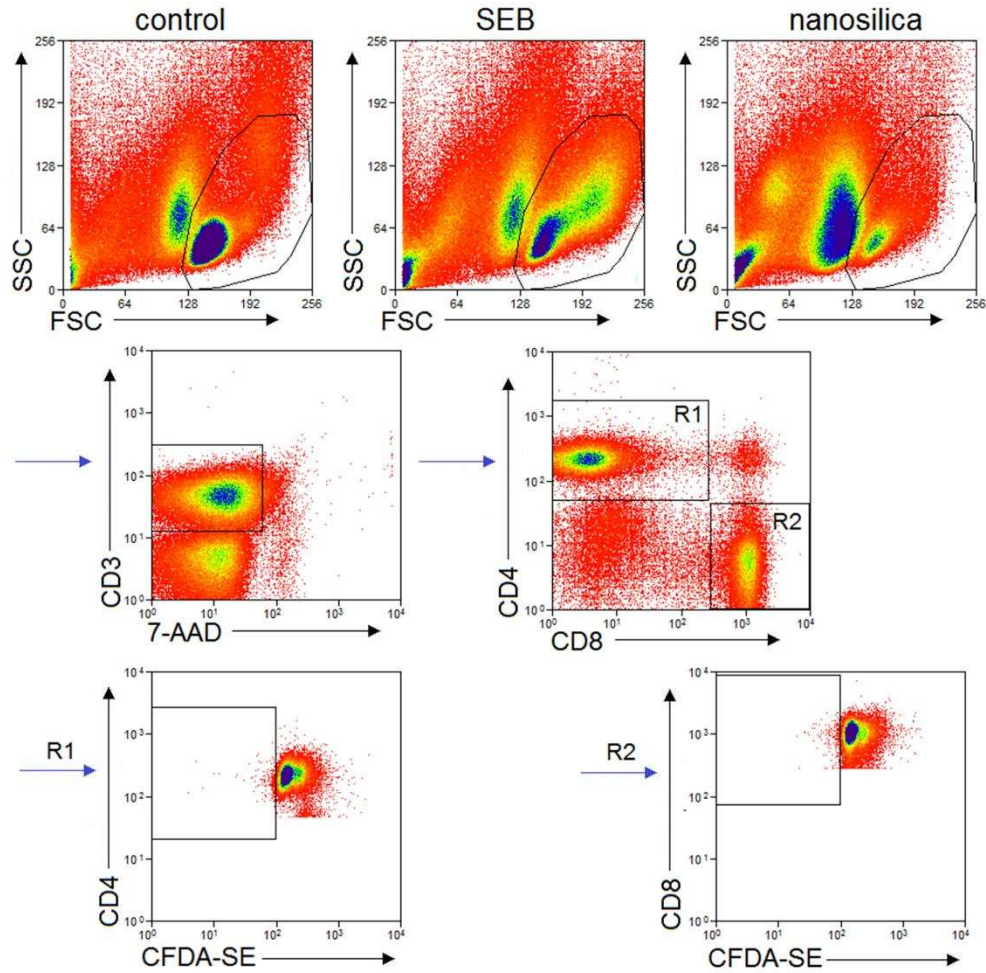


Figure S7. Gating strategy employed for assessing CD69 on Jurkat cells

Cells were first selected based on a FSC versus SSC profile that excluded debris, followed by a viable T cell (CD3(+)). Percentage of cells positive for CD69 was plotted against the SSC profile.

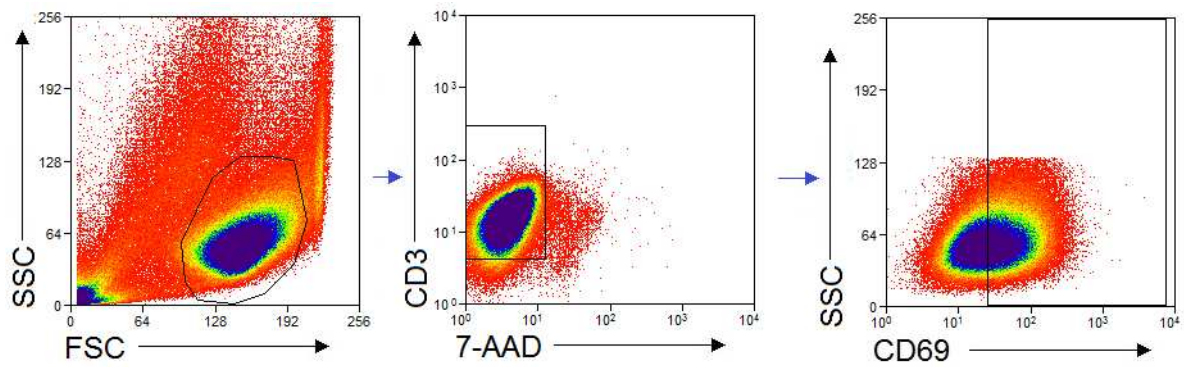


Table S1.

USSN zeta-potential and derived count rate in PBS and RPMI. Although USSN-free PBS and RPMI both contained species with zeta-potentials similar to the USSN containing media, the derived count rate (kcps), which is a measure of particle density based on scattering intensity, of the media containing USSN was higher than the USSN-free media. This indicated that particles were detected in the complex media, and the zeta-potentials correspond to that of the USSN. The decrease in charge magnitude in the complex media versus ultrapure water (UHP) is consistent with trends reported in the literature.²

	Zeta-potential /mV	kcps
PBS	-22.4±0.9	222 +/- 22
PBS + USSN	-19.0 ± 4.4	1436 ± -519
RPMI	-11.2+/-1.6	29.0+/-7.8
RPMI + USSN	-16.0 ± 1.9	356 ± 89

Table S2.

The 100 gene pathways which are most significantly up regulated in PBMC culture by 150 μ M USSN.

NAME	SIZE	NES	FDR q-val
KEGG_LYSOSOME	122	2.412125	0
TRANSFERRIN.ENDOCYTOSIS.AND.RECYCLING	29	2.34737	0
KEGG_COLLECTING.DUCT.ACID.SECRETION	27	2.332215	0
IRON.UPTAKE.AND.TRANSPORT	43	2.306844	0
WP2670.IRON.UPTAKE.AND.TRANSPORT	112	2.278574	0
WP2700.LATENT.INFECTION.OF.HOMO.SAPIENS.WITH.MYCOBACTERIUM.TUBERCULOSIS	30	2.270007	0
LATENT.INFECTION.OF.HOMO.SAPIENS.WITH.MYCOBACTERIUM.TUBERCULOSIS	33	2.214397	2.09E-04
PHAGOSOMAL.MATURATION.EARLY.ENDOSOMAL.STAGE.	33	2.227816	2.35E-04
INSULIN.RECEPTOR.RECYCLING	26	2.233781	2.69E-04
SPHINGOLIPID.METABOLISM	69	2.148967	3.84E-04
KEGG_SPHINGOLIPID.METABOLISM	47	2.031814	0.006816
GLYCOSPHINGOLIPID.METABOLISM	38	2.014864	0.007862
KEGG_VIBRIO.CHOLERAЕ.INFECTION	54	1.996895	0.008833
WP516.HYPERTROPHY.MODEL	20	1.977822	0.010697
KEGG_SYNAPTIC.VESICLE.CYCLE	63	1.981199	0.010844
P75NTR.SIGNALS.VIA.NF.KB	15	1.934304	0.017494
WP197.CHOLESTEROL.BIOSYNTHESIS	17	1.93623	0.018041
WP1913.SIGNALING.BY.INSULIN.RECEPTOR	73	1.923677	0.018852
WP2788.SPHINGOLIPID.METABOLISM	45	1.899784	0.023461
KEGG_RHEUMATOID.ARTHRITIS	86	1.864963	0.034792
WP530.CYTOKINES.AND.INFLAMMATORY.RESPONSE	23	1.84501	0.043395
MPS.VI.MAROTEAUХ.LAMY.SYNDROME	120	1.711475	0.075753
GLYCOSAMINOGLYCAN.METABOLISM	120	1.715812	0.075788
MPS.IX.NATOWICZ.SYNDROME	120	1.70496	0.076394
MPS.I.HURLER.SYNDROME	120	1.712378	0.07667
DEFECTIVE.EXT2.CAUSES.EXOSTOSES.2	120	1.716062	0.077156
DEFECTIVE.PAPSS2.CAUSES.SEMD.PA	120	1.705239	0.077593
WP1795.CHOLESTEROL.BIOSYNTHESIS	19	1.706618	0.077975
DEFECTIVE.B3GAT3.CAUSES.JDSSDHD	120	1.716364	0.078503
MPS.IV.MORQUIO.SYNDROME.B	120	1.718244	0.078998
MPS.IIIC.SANFILIPPO.SYNDROME.C	120	1.697702	0.079648
MUCOPOLYSACCHARIDOSES	120	1.719842	0.079703
COLLAGEN.DEGRADATION	38	1.699164	0.079853
DEFECTIVE.CHST14.CAUSES.EDS.MUSCULOCONTRACTURAL.TYPE	120	1.721098	0.080256
DEFECTIVE.EXT1.CAUSES.EXOSTOSES.1.TRPS2.AND.CHDS	120	1.721384	0.08195
BIOC_41BBPATHWAY	18	1.69045	0.082406
MPS.VIISLY.SYNDROME	120	1.7231	0.08247
AMINO.ACID.AND.OLIGOPEPTIDE.SLC.TRANSPORTERS	49	1.690767	0.083641
DEFECTIVE.CHST3.CAUSES.SEDCJD	120	1.723611	0.083878
GAP.JUNCTION.ASSEMBLY	17	1.725111	0.084567
SPHINGOLIPID.DE.NOVO.BIOSYNTHESIS	31	1.683833	0.084691
MPS.IIIB.SANFILIPPO.SYNDROME.B	120	1.729995	0.085017
MPS.IIID.SANFILIPPO.SYNDROME.D	120	1.727214	0.085172
GAP.JUNCTION.TRAFFICKING.AND.REGULATION	28	1.685041	0.085179
DEFECTIVE.SLC26A2.CAUSES.CHONDRODYSPLASIAS	120	1.730998	0.08641
MPS.IIHUNTER.SYNDROME	120	1.732043	0.088056
SIGNALING.BY.INSULIN.RECEPTOR	115	1.781837	0.088196
DISEASES.ASSOCIATED.WITH.GLYCOSAMINOGLYCAN.METABOLISM	120	1.732122	0.090393
KEGG_AMINO.SUGAR.AND.NUCLEOTIDE.SUGAR.METABOLISM	47	1.77501	0.091561
WP2011.SREBF.AND.MIR33.IN.CHOLESTEROL.AND.LIPID.HOMEOSTASIS	17	1.673107	0.091951
DEFECTIVE.B4GALT1.CAUSES.B4GALT1.CDG.CDG.2D.	120	1.732738	0.092308
MPS.IV.MORQUIO.SYNDROME.A	120	1.745403	0.092365
MPS.IIIA.SANFILIPPO.SYNDROME.A	120	1.733872	0.09394
DEFECTIVE.CHSY1.CAUSES.TPBS	120	1.749261	0.094602
CHEMOKINE.RECEPTORS.BIND.CHEMOKINES	53	1.745979	0.094671
WP430.STATIN.PATHWAY	29	1.666234	0.096101
DEFECTIVE.B4GALT7.CAUSES.EDS.PROGEROID.TYPE	120	1.734324	0.096461
KERATAN.SULFATE.KERATIN.METABOLISM	32	1.766427	0.096475
KERATAN.SULFATE.BIOSYNTHESIS	27	1.76192	0.096898
KEGG_EPITHELIAL.CELL.SIGNALING.IN.HELICOBACTER.PYLORI.INFECTION	68	1.749733	0.097562
WP2840.HAIR.FOLLICLE.DEVELOPMENT.CYTODIFFERENTIATION.PART.3.OF.3.	86	1.661783	0.098289
DISEASES.OF.GLYCOSYLATION	120	1.735025	0.09893
DEFECTIVE.CHST6.CAUSES.MCDC1	120	1.754486	0.100371
GAP.JUNCTION.TRAFFICKING	26	1.750262	0.100669
KEGG_RIBOSOME.BIOGENESIS.IN.EUKARYOTES	72	1.640219	0.116826
BIOC_IL1RPATHWAY	32	1.620022	0.138707
WP706.SIDS.SUSCEPTIBILITY.PATHWAYS	154	1.614106	0.144288
BIOC_INFLAMPATHWAY	29	1.606008	0.152143
KEGG_STEROID.BIOSYNTHESIS	20	1.602853	0.153887
INTERACTION.BETWEEN.L1.AND.ANKYRINS	29	1.59329	0.159489
BASIGIN.INTERACTIONS	25	1.593826	0.160913
KEGG_OTHER.GLYCAN.DEGRADATION	18	1.589595	0.162257
PERK.REGULATES.GENE.EXPRESSION	28	1.594093	0.162766
KEGG_CIRCADIAN.RHYTHM	30	1.580349	0.172092
WP195.IL.1.SIGNALING.PATHWAY	56	1.578051	0.173034
BIOC_EDG1PATHWAY	22	1.565499	0.188346
KEGG_CYTOKINE.CYTOKINE.RECEPTOR.INTERACTION	258	1.556644	0.199329
FGFR.LIGAND.BINDING.AND.ACTIVATION	23	1.536761	0.221117
WP2855.DOPMINERGIC.NEUROGENESIS	30	1.534687	0.22201
WP1867.NEPHRIN.INTERACTIONS	19	1.539006	0.222848
WP236.ADIPOGENESIS	131	1.537218	0.223171
OXYGEN.DEPENDENT.PROLINE.HYDROXYLATION.OF.HYPOXIA.INDUCIBLE.FACTOR.ALPHA	17	1.539057	0.225593
KEGG_BILE.SECRETION	72	1.528364	0.227608
WP1422.SPHINGOLIPID.METABOLISM	21	1.528405	0.230257
SIGNALING.BY.FGFR.MUTANTS	45	1.524603	0.231493
WP1471.TOR.SIGNALING	34	1.520902	0.23543
KEGG_SELENOCOMPOUND.METABOLISM	17	1.511018	0.250376
BIOC_GSK3PATHWAY	26	1.507782	0.253781
SIALIC.ACID.METABOLISM	33	1.505087	0.256066
BUDDING.AND.MATURATION.OF.HIV.VIRION	23	1.501416	0.260283
AMINO.ACID.TRANSPORT.ACROSS.THE.PLASMA.MEMBRANE	31	1.491757	0.276207

KEGG_GLYCOSAMINOGLYCAN.BIOSYNTHESIS.CHONDROITIN.SULFATE.DERMATAN.SULFATE	20	1.48673	0.280231
WP2003.MIR.TARGETED.GENES.IN.LEUKOCYTES.TARBASE	150	1.488119	0.280555
SIGNALING.BY.FGFR1.MUTANTS	30	1.483293	0.284049
WP2037.PROLACTIN.SIGNALING.PATHWAY	77	1.478202	0.284943
WP1982.SREBP.SIGNALING	63	1.47823	0.287829
WP615.SENESCENCE.AND.AUTOPHAGY	106	1.478805	0.289463
KEGG_INFLAMMATORY.BOWEL.DISEASE.IBD.	63	1.473289	0.291857
WP428.WNT.SIGNALING.PATHWAY	60	1.470805	0.294348
WP2743.GLYCOSAMINOGLYCAN.METABOLISM	41	1.462832	0.299421

Table S3.

The 100 gene pathways which are most significantly down regulated in PBMC culture by 150 μM USSN.

NAME	SIZE	NES	FDR q-val
PEROXISOMAL.LIPID.METABOLISM	21	-2.05276	0.042144
KEGG_PEROXISOME	79	-2.02518	0.038501
HDACS.DEACETYLATE.HISTONES	56	-2.00952	0.032493
WP1878.PEROXISOMAL.LIPID.METABOLISM	19	-1.91423	0.083207
ANTIGEN.ACTIVATES.B.CELL.RECEPTOR.BCR.LEADING.TO.GENERATION.OF.SECOND.MESSENGERS	37	-1.88025	0.106366
BIOC_AMIPATHWAY	21	-1.84779	0.136954
SCAVENGING.OF.HEME.FROM.PLASMA	18	-1.83125	0.144034
THE.CITRIC.ACID.TCA.CYCLE.AND.RESPIRATORY.ELECTRON.TRANSPORT	135	-1.81789	0.148693
BIOC_CSKPATHWAY	21	-1.81738	0.133181
RNA.POLYMERASE.I.PROMOTER.OPENING	24	-1.78007	0.180335
REGULATION.OF.ACTIN.DYNAMICS.FOR.PHAGOCYTIC.CUP.FORMATION	63	-1.77775	0.168337
WP2675.SIGNALING.BY.NODAL	15	-1.76286	0.18134
PLATELET.SENSITIZATION.BY.LDL	17	-1.74141	0.211196
IMMUNOREGULATORY.INTERACTIONS.BETWEEN.A.LYMPHOID.AND.A.NON.LYMPHOID.CELL	72	-1.71614	0.255837
ACYL.CHAIN.REMODELLING.OF.PS	16	-1.71467	0.241663
PACKAGING.OF.TELOMERE.ENDS	27	-1.70624	0.249746
CONDENSATION.OF.PROPHASE.CHROMOSOMES	34	-1.69391	0.265173
BIOC_MCALPAINPATHWAY	24	-1.69047	0.257973
KEGG_BASE.EXCISION.REPAIR	33	-1.68799	0.249315
NUCLEOSOME.ASEMBLY	41	-1.68523	0.243609
WP1433.NOD.PATHWAY	39	-1.68515	0.232154
WP1848.METABOLISM.OF.CARBOHYDRATES	85	-1.68274	0.227145
DEPOSITION.OF.NEW.CENPA.CONTAINING.NUCLEOSOMES.AT.THE.CENTROMERE	41	-1.68183	0.218699
FORMATION.OF.ATP.BY.CHEMIOSMOTIC.COUPLING	16	-1.6764	0.220682
RESPIRATORY.ELECTRON.TRANSPORT.ATP.SYNTHESIS.BY.CHEMIOSMOTIC.COUPLING.AND.HEAT.PRODUCTI ON.BY.UNCOUPLING.PROTEINS	94	-1.66472	0.237673
WP111.ELECTRON.TRANSPORT.CHAIN	90	-1.66452	0.228766
REGULATION.OF.PYRUVATE.DEHYDROGENASE.PDH.COMPLEX	16	-1.66333	0.223145
PYRUVATE.METABOLISM.AND.CITRIC.ACID.TCA.CYCLE	45	-1.66166	0.219033
GENERATION.OF.SECOND.MESSENGER.MOLECULES	31	-1.65857	0.217164
SIGNALING.BY.NODAL	16	-1.64284	0.240378
FCER1.MEDIATED.NF.KB.ACTIVATION	29	-1.63362	0.250823
BIOC_MPRPATHWAY	22	-1.63278	0.24436
BIOC_BCRPATHWAY	34	-1.62084	0.262697
WP1874.NUCLEOSOME.ASEMBLY	32	-1.60829	0.284836
CHROMOSOME.MAINTENANCE	76	-1.60825	0.276757
KEGG_PRIMARY.IMMUNODEFICIENCY	36	-1.60526	0.276278
INTEGRIN.ALPHA.IB.BETA.3.SIGNALING	27	-1.60495	0.269673
ABCA.TRANSPORTERS.IN.LIPID.HOMEOSTASIS	17	-1.60061	0.27235
WP623.OXIDATIVE.PHOSPHORYLATION	52	-1.59607	0.275946
WP2739.AMYLOIDS	24	-1.58423	0.296655
WP500.GLYCOGEN.METABOLISM	36	-1.58115	0.296425
WP1902.RESPIRATORY.ELECTRON.TRANSPORT.ATP.SYNTHESIS.BY.CHEMIOSMOTIC.COUPLING.AND.HEAT.PR ODUCTION.BY.UNCOUPLING.PROTEINS	81	-1.5802	0.291377
WP2775.TOLL.LIKE.RECEPTORS.CASCADES	23	-1.57186	0.305471
DNA.DAMAGE.TELOMERE.STRESS.INDUCED.SENESCENCE	54	-1.5697	0.303974
RESOLUTION.OF.SISTER.CHROMATID.COHESION	98	-1.56646	0.305041
REV.ERBA.REPRESSES.GENE.EXPRESSION	24	-1.56555	0.300687
FCGAMMA.RECEPTOR.FCGR.DEPENDENT.PHAGOCYTOSIS	87	-1.56021	0.306386
GENERIC.TRANSSCRIPTION.PATHWAY	469	-1.56001	0.300578
BIOC_ERKSPATHWAY	16	-1.55516	0.306077
BIOC_HIVNEFPATHWAY	53	-1.55135	0.309209
BIOC_CREBPATHWAY	26	-1.54902	0.309215
YAP1.AND.WWTR1.TAZ.STIMULATED.GENE.EXPRESSION	29	-1.54817	0.305485
PD.1.SIGNALING	22	-1.54028	0.317824
KEGG_DNA.REPLICATION	36	-1.53943	0.314255
TRANSLOCATION.OF.ZAP.70.TO.IMMUNOLOGICAL.SYNAPSE	17	-1.53782	0.312487
WP408.OXIDATIVE.STRESS	29	-1.53738	0.307894
RORA.ACTIVATES.CIRCADIAN.GENE.EXPRESSION	25	-1.53584	0.306121
SYNTHESIS.OF.IP3.AND.IP4.IN.THE.CYTOSOL	25	-1.53332	0.306392
WP1829.IMMUNOREGULATORY.INTERACTIONS.BETWEEN.A.LYMPHOID.AND.A.NON.LYMPHOID.CELL	59	-1.53216	0.304031
PLC.BETA.MEDIATED.EVENTS	42	-1.52691	0.311906
WP1978.OPIOID.SIGNALING	57	-1.52546	0.310316
WP1928.TELOMERE.MAINTENANCE	45	-1.52543	0.30536
SIRT1.NEGATIVELY.REGULATES.RRNA.EXPRESSION	29	-1.52512	0.301215
WP2652.MITOTIC.PROMETAPHASE	95	-1.51659	0.316351
WP2371.PARKINSONS.DISEASE.PATHWAY	38	-1.51089	0.32578
PHOSPHORYLATION.OF.CD3.AND.TCR.ZETA.CHAINS	19	-1.51016	0.322471
MITOTIC.PROMETAPHASE	106	-1.5097	0.318636
ROLE.OF.PHOSPHOLIPIDS.IN.PHAGOCYTOSIS	30	-1.50869	0.316672
KEGG_GLUTATHIONE.METABOLISM	48	-1.50852	0.312469
ACYL.CHAIN.REMODELLING.OF.PI	16	-1.50372	0.318654
BIOC_TNFR1PATHWAY	28	-1.50309	0.315698
RESPIRATORY.ELECTRON.TRANSPORT	75	-1.50092	0.316559
WP1832.INTEGRIN.ALPHA.IB.BETA.3.SIGNALING	19	-1.49918	0.316779
KEGG_PROPANOATE.METABOLISM	28	-1.49915	0.312583
WP2795.CARDIAC.HYPERTROPHIC.RESPONSE	56	-1.49899	0.30885
KEGG_ALCOHOLISM	165	-1.49891	0.304936
BIOC_SPPAPATHWAY	21	-1.49784	0.303693
BIOC_ERKPATHWAY	29	-1.49495	0.306755
RNA.POLYMERASE.I.TRANSCRIPTION	69	-1.49322	0.306817
KEGG_HUNTINGTON.S.DISEASE	183	-1.49081	0.308532
RNA.POLYMERASE.I.PROMOTER.CLEARANCE	67	-1.48917	0.308396
KEGG_SHIGELLOSIS	60	-1.48731	0.308748
WP304.KIT.RECEPTOR.SIGNALING.PATHWAY	59	-1.48286	0.315417
MEIOTIC.SYNAPSIS	53	-1.48264	0.312235
WP364.IL.6.SIGNALING.PATHWAY	43	-1.48168	0.310832
KEGG_FANCONI.ANEMIA.PATHWAY	49	-1.47277	0.327754
G.PROTEIN.MEDIATED.EVENTS	43	-1.46968	0.331187
WP1980.NUCLEOTIDE.EXCISION.REPAIR	47	-1.46758	0.33237
WP1787.BASE.EXCISION.REPAIR	19	-1.4642	0.335958

KEGG_PARKINSON.S.DISEASE	128	-1.45984	0.342553
WP1885.PLATELET.HOMEOSTASIS	28	-1.45976	0.339025
KEGG_FC.GAMMA.R.MEDIATED.PHAGOCYTOSIS	88	-1.45944	0.33639
FORMATION.OF.THE.BETA.CATENIN.TCF.TRANSACTIVATING.COMPLEX	52	-1.45682	0.338852
WP23.B.CELL.RECEPTOR.SIGNALING.PATHWAY	93	-1.45426	0.341527
WP422.MAPK.CASCADE	29	-1.45415	0.338257
KEGG_VALINE.LEUCINE.AND.ISOLEUCINE.DEGRADATION	43	-1.45321	0.337081
KEGG_GLYOXYLATE.AND.DICARBOXYLATE.METABOLISM	24	-1.453	0.33403
RAP1.SIGNALLING	16	-1.44899	0.340437
KEGG_GLYCOSYLPHOSPHATIDYLINOSITOL.GPI.ANCHOR.BIOSYNTHESIS	24	-1.44642	0.343097
DNA.METHYLATION	26	-1.44597	0.340753

References

1. Jelfs, K. E.; Flikkema, E.; Bromley, S. T., Hydroxylation of Silica Nanoclusters $(\text{SiO}_2)_M(\text{H}_2\text{O})_N$, $M= 4, 8, 16, 24$: Stability and Structural Trends. *Phys. Chem. Chem. Phys.* **2013**, *15*, 20438-20443
2. Kobayashi, M.; Juillerat, F.; Galletto, P.; Bowen, P.; Borkovec, M., Aggregation and Charging of Colloidal Silica Particles: Effect of Particle Size. *Langmuir* **2005**, *21*, 5761-5769.